Mg/Al-CH, Ni/Al-CH, and Zn/Al-CH as adsorbents for Congo Red removal in aqueous solution

Patimah Mega Syah Bahar Nur Siregar[a], Normah[a], Novie Juleanti[a], Alfan Wijaya[a], Neza Rahayu Palapa[b], Risfidian Mohadi[b], Aldes Lesbani[b,c,*]

[a]*Magister Programme Graduate School of Mathematics and Natural Sciences, Universitas Sriwijaya, Palembang 30139, Indonesia*

[b]*Graduate School, Faculty of Mathematics and Natural Sciences, Universitas Sriwijaya, Palembang 30139, Indonesia*

[c]*Research Center of Inorganic Materials and Complexes, Faculty of Mathematics and Natural Sciences, Universitas Sriwijaya, Palembang 30139, Indonesia*

Abstract

In this study, chitosan was extracted from shrimp shells by demineralization and deproteination processes. The extracted chitosan was used to modify the layered double hydroxide and used as an adsorbent for the removal of congo red from aqueous solutions. Composites were successfully synthesized using M^{2+}/Al (M^{2+} = Zn, Mg, Ni) and chitosan (CH) and the samples obtained were characterized using XRD and FTIR. The X-ray diffraction (XRD) pattern appeared at the layered double hydroxide peak of 2θ = 11.63°; 23.00°; 35.16°; and 61.59° and chitosan at 2θ = 7.93° and 19.35. The composite appearing in the layered double hydroxide and chitosan indicated that the composite material has been successfully synthesized. The XRD diffraction patterns of Zn/Al-CH, Ni/Al-CH, and Mg/Al-CH showed low crystallinity. The Fourier Transform Infrared (FTIR) spectra verifying absorption spectrum showed the presence of two bands at 3448 cm^{-1}, 1382cm^{-1} characteristic to both chitosan and LDH. Adsorption of Congo Red (CR) followed the pseudo-second-order and Langmuir isotherm models. The adsorption capacities of Zn/Al-CH, Ni/Al-CH, and Mg/Al-CH were 181.818 mg/g, 227.273 mg/g, and 344.828 mg/g, respectively. The layered double hydroxide-chitosan composite adsorption was endothermically characterized by positive enthalpy and entropy values. On the other hand, the adsorption spontaneously was characterized by a negative Gibbs free energy value. The composites in this study were formed from LDH modified from chitosan extracted from shrimp shells to form Zn/Al-CH, Ni/Al-CH, and Mg/Al-CH. The results of the characterization showed a number of characteristics that resembled the constituent materials in the form of LDH and chitosan. After being applied as an adsorbent to absorb Congo red dye, it then showed the most effective results using Mg/Al-CH adsorbent with an adsorption capacity of 344.828 mg/g.

Keywords: Chitosan; selectivity; adsorption; regeneration

1. Introduction

The use of synthetic dyes in textile industry has some positive impacts in regard to higher durability, stability and more color variations [1]. However, the waste of synthetic dye has a number of negative impacts, in terms of environmental pollution. Synthetic dyestuffs can also be degraded into carcinogenic [2] and toxic compounds. Congo Red or CR is a reactive dye that is widely used in the textile industry [3]. It is an aromatic complex compound, red with the molecular formula ($C_{32}H_{22}N_6Na_2O_6S_2$) [4]. The existence of CR dye in the environment can have some quite serious impacts for living because the nature of CR toxicity is quite high and it can cause the disorders of liver [5], nerves, and kidneys when entering the body [6].

Some efforts need to be given to minimize Congo red dye waste before being discharged into the waters considering its effects. Several methods can be used to minimize the dye content in textile industry waste, including coagulation [7],

electrocoagulation, photodegradation, ozonation [8], biodegradation [9], electrolysis, and oxidation methods. However, these methods are less effective in dealing with textile dye waste and often arise some problems for the environment. Adsorption is the most common method used to treat waste with affordably [10] and simply in its operation [11]. Also adsorbent can be used again (regeneration) [12]. Several factors affect adsorption such as the type of adsorbent used, contact time, pH, and weight. The use of affordable and environmentally friendly adsorbents is needed to minimize the cost of the adsorption process.
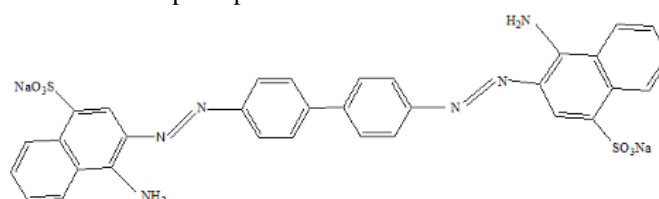

Figure. 1. Chemical Structure of CR

Chitosan (CH) is a natural polymer in the form of a yellowish-white amorphous solid and is a polyelectrolyte with a molecular weight of 120,000 g/mol. Chitosan (poly-β-(1→4)-

2-amino-2-deoxy-D-glucose, or D-Glucosamine, or a compound with the formula $(C_6H_{11}NO_4)n$ is a reactive cationic polymer compound of amino acids [13], namely amino polysaccharides [14]. Chitosan contains an amino group ($-NH_2$) and hydroxyl group ($-OH$) enabling it to be potential as an adsorbent for cationic and anionic dyestuffs and heavy metals [15]. However, it has a small surface area, so it needs to be modified for more effective results. Chitosan can be modified physically or chemically to reduce particle size and expand the surface of chitosan by composite, grafting, and crosslinking. The poor physical properties of chitosan can be improved if it is composited on the clay/clay surface. The coating of chitosan as a thin layer on the clay supports to increase the ease of binding and improve the mechanical stability of chitosan.

Chitosan can be obtained from crustacean waste such as shrimp and crabs. The choice of chitosan as an adsorbent in addition to utilizing waste is also because it is cheap, biodegradable, biocompatible and having high selectivity. Chitosan is also easily formed into materials in the form of films, membranes, tissues, sponges, gels, beads, and nanoparticles. However, the direct use of chitosan as an adsorbent is less effective as it has low chemical stability, is easily biodegradable and easily soluble in acids such as HNO_3, CH_3COOH, and HCl.

In this study, composites were made using layered double hydroxides (LDH) M^{2+}/Al ($M^{2+}=$ Mg, Ni, Zn) and chitosan. Mg/Al-CH, Ni/Al-CH, and Zn/Al-CH were used to remove CR from aqueous solutions. The obtained materials were then characterized using XRD and FTIR. To determine the adsorption ability of composites, it was studied through the selection of a mixture of dyes, isotherms, and adsorption thermodynamics, as well as adsorption regeneration studies.

2. Materials and Methods

2.1. Chemicals and instrumentation

In this work, materials included $Mg(NO_3)_2.6H_2O$ (EMSURE® ACS, 256.41 g/mol), $Ni(NO_3)_2.6H_2O$ (EMSURE® ACS, 290.81 g/mol, $Zn(NO_3)_2.6H_2O$ (297.49 g/mol) $Al(NO_3)_3.9H_2O$ (Sigma-Aldrich, 375.13 g/mol), NaOH (EMSURE® ISO, 40 g/mol), distilled water (PT. Bratachem Indonesia), malachite green (MG), methylene blue (MB), and congo red (CR). CH was extracted from shrimp shells by demineralization and deproteination [13]. The material was characterized by X-Ray Rigaku Miniflex-6000, FTIR using Shimadzu Prestige-21. The concentration of dye was measured using a UV-Visible spectrophotometer Bio-Base BK-UV1800.

2.2. Preparation of composite M^{2+}/Al (M^{2+} = Mg, Ni, Zn)

The M^{2+} solution is $Mg(NO_3)_2.6H_2O$, $Ni(NO_3)_2.6H_2O$, $Zn(NO_3)_2.6H_2O$ and Al^{3+} solution = $Al(NO_3)_3.9H_2O$ with a molar ratio of 3:1. The mixture was dripped with NaOH to pH 10 and the suspension was stirred for 1 hour to form a layered structure. In the final process, the suspension was added with 3 g of chitosan into each layered double hydroxide (Mg/Al, Ni/Al, and Zn/Al) and stirred for 72 hours using a temperature of 70°C. After 72 hours, the suspension was filtered using the vacuum to obtain residue, rinsed with distilled water, and dried in an oven at 50°C. The material was characterized using XRD and FTIR.

2.3. Selectivity of Dyes

The selectivity of the dyes mixture was carried out by mixing cationic dyes (MB, MG) and anionic dyes (CR) with a dye concentration of 20 mg/L each and 0.02 g adsorbent (Mg/Al-CH, Ni/Al-CH, and Zn/Al-CH). The dye mixture was stirred according to the variation of time used (0, 15, 30, 60, and 120 minutes). Here, the dye mixture was measured using a UV-Visible spectrophotometer.

2.4. pH optimum of Congo Red

The pH variation of the dye was carried out using a concentration of 50 mg/L Congo red with a pH variation of 2, 3, 4, 5, 6, 7, 8, 9, 10, and 11, using HCl and NaOH in the setting process. Then, 0.02 g of adsorbent was added to the solution and stirred for 2 hours. The separation process was carried out by centrifugation and the obtained filtrate was measured for its absorbance value using a UV-Vis Spectrophotometer.

2.5. Adsorption Process

The effect of isotherm and adsorption thermodynamics was determined by varying the initial concentrations of CR (60, 70, 80, 90, and 100 mg/L) and adsorption temperatures (60, 70, 80, 90, and 100°C). The filtrate was measured using a UV-Visible spectrophotometer at a wavelength of 466 nm.

2.6. Regeneration of Adsorbent

The structural stability of Zn/Al-CH, Mg/Al-CH, and Ni/Al-CH was evaluated by the dyes regeneration process after desorption using an ultrasonic system. The regeneration process of each adsorbent was carried out by adsorbing dyes on each adsorbent. The dyes concentration of 100 mg/L was as much as 25 mL and each adsorbent of 0.1 g. The adsorbent after dyes adsorption was desorbed by an ultrasonic system equipped with a water chamber and then the adsorbent was dried at 100°C for 3 hours. After the adsorption process was complete, the absorbance of dyes was measured. The adsorbent used was filtered and then dried to make it possible to be used for seven regenerations. The regeneration process was carried out until the adsorbent were not able to re-adsorb so that in this study the regeneration process was carried out for 7 cycles [17].

3. Results and Discussion

Figure 2 shows the diffraction pattern of the LDH-based composite and chitosan support material. Composites can be stated as a combination of two or more constituent materials where the chemical and physical properties are different and remain separate in the final product of the material [18]. Figures a, b, and c show diffraction at an angle of $2\theta = 11.63°$ (003); 23.00° (006); 35.16° (009); and 61.59° (110) as the typical peak of LDH. The characteristic peak of chitosan appears at an angle of 7.93° and 19.35°, indicating that the chitosan is semi-crystalline [15].

Figure 3 (a, b, c) shows the vibrational peak of LDH at the wavenumber of 3464 cm⁻¹ indicating the presence of O-H vibrations of water molecules. The peak of the vibration at wavenumber 1635 cm⁻¹ indicated a bending vibration of O-H. The peak of the vibration at wavenumber 1381 cm⁻¹ indicated the existence of vibration from the NO_3^- anion and the peak of the vibration at the wavenumber of 748 cm⁻¹ was the M-O vibration in the form of Ni-O and Al-O [4]. Figure 3(d) shows the vibrational peak at 3427 cm⁻¹ (O-H group of chitosan), 2924 and 2870 cm⁻¹ (C-H stretch) , 1566 cm⁻¹ and (C=C stretch of aromatic ring) [19]. Zn/Al-CH, Mg/Al-CH, and Ni/Al-CH composite (Figure 3 e, f, g), the absorption spectrum shows the presence of two bands at 3448, 1382 cm⁻¹ characteristic to both chitosan and LDH. A shift occurred in the peak at 1654 cm⁻¹ was due to the υ_3 vibration of NO_3^- [20].
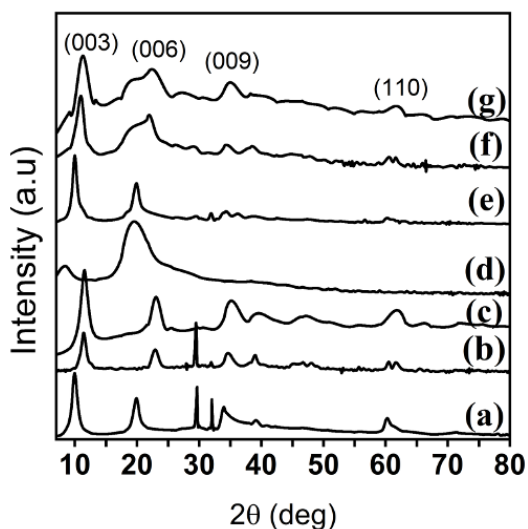

Figure. 2. XRD powder patterns of Zn/Al LDH (a), Mg/Al LDH (b), Ni/Al-LDH (c), Chitosan (d), Zn/Al-CH ©, Mg/Al-CH (f), and Ni/Al-CH (g)

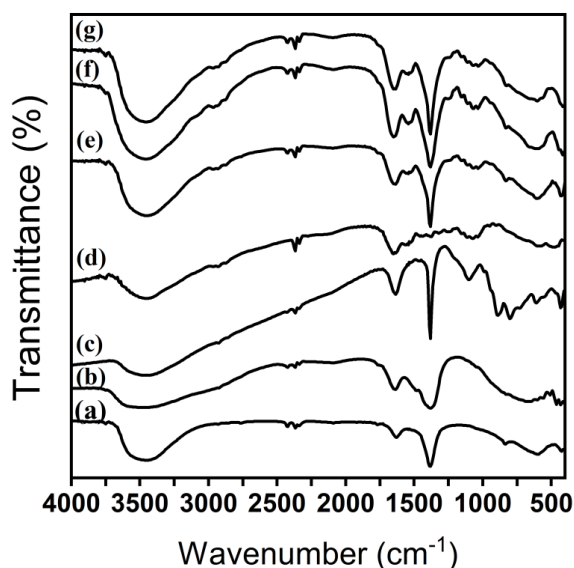

Figure 3. FTIR spectrum of Zn/Al LDH (a), Mg/Al LDH (b), Ni/Al-LDH (c), Chitosan (d), Zn/Al-CH ©, Mg/Al-CH (f), and Ni/Al-CH (g)

Figure 4 shows the dye selectivity of each adsorbent. The selectivity process was carried out by measuring the maximum wavelength of the dye mixture methylene blue (MB), malachite green (MG), and Congo Red (CR) using wavelengths in the range of 400 to 700nm. The selectivity of the dye mixture can be seen from the change in the maximum wavelength during the adsorption process at a predetermined time variation. There was a decrease in the absorbance of each mixture as the adsorption time increased. Figure 4 shows a drastic decrease in absorbance occurred at 120 minutes and it can be seen that CR dyes were more effectively adsorbed than MB and MG. Then the isotherm adsorption process and thermodynamic adsorption on the most selective dyes were carried out.
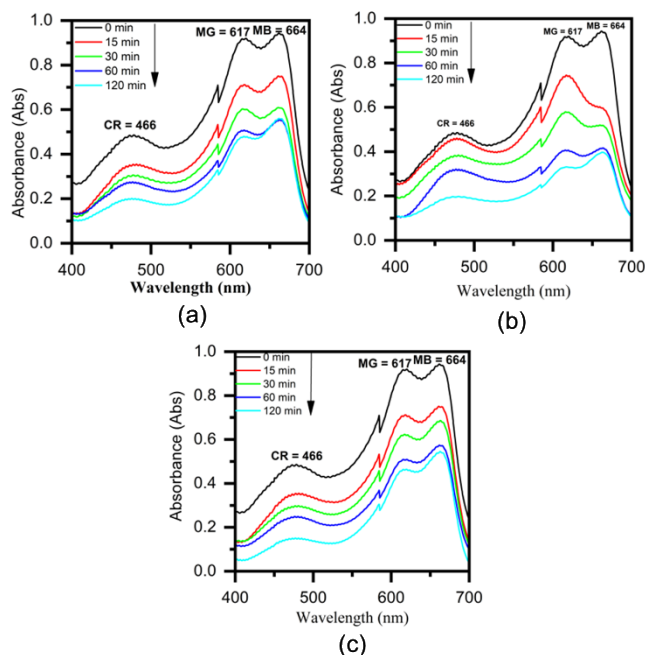

Figure 4. UV-Visible spectra of mixture MB, MG, and CR onto Zn/Al-CH (a), Ni/Al-CH (b), and Mg/Al-CH (c)
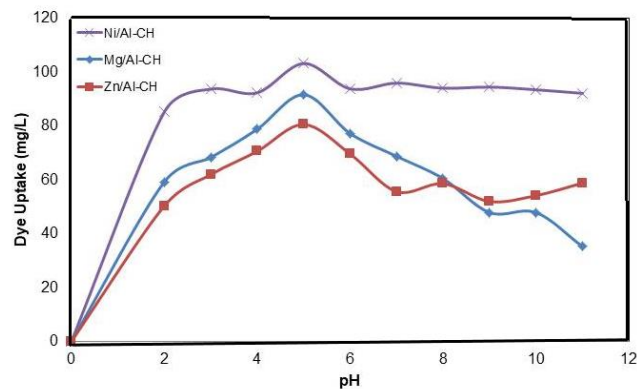

Figure 5. pH optimum of CR using Zn/Al-CH, Mg/Al-CH, and Ni/Al-CH

Figure 5 shows the optimum pH of the CR of each adsorbent. The pH will have a direct impact on changes in the wavelength of the CR dye. Adsorption is influenced by pH, by affecting the protonation of the adsorbent used. Each adsorbent will have a different charge so that they can interact with each other. Under acidic conditions, the dye will be deprotonated and when the adsorbent is added to the dye solution, the surface of the adsorbent will be protonated first and then electrostatic interactions will occur and cause the transfer of the dye in the solution to the surface of the protonated adsorbent.

The determination of the adsorption kinetics of CR was studied by varying the time (0, 10, 20, 30, 40, 50, 60, 70, 90,

120, 150, 180, and 200 minutes) as shown in Figure 6. The closer the R^2 values to 1, the better the adsorption process. The value of the adsorption rate constant (k) is an adsorption kinetics parameter that indicates fast or slow process of the adsorption [21]. The higher the value of k, the faster the adsorption takes place. The value of Qe is the amount of CR adsorbed at equilibrium. The higher the value of Qe, the higher the amount of substance adsorbed. Table 1 shows the effect of contact time; the R^2 value tends to follow *pseudo-second-order* for each adsorbent used, judging from the R^2 value closer to 1.
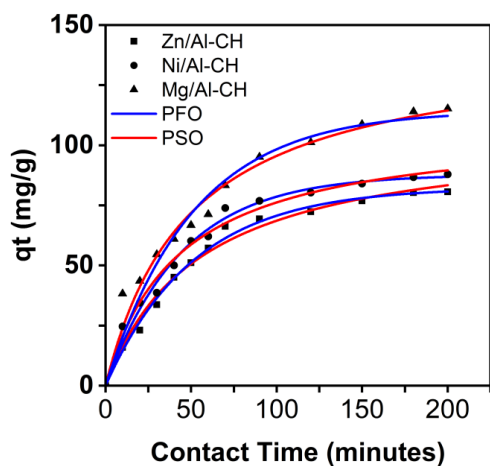

Figure 6. Time variation of adsorption

Table 1. Kinetic parameter

Adsorbent	Initial Concentration (mg/L)	Qe_{exp} (mg/g)	PFO			PSO		
			Qe_{Calc} (mg/g)	R^2	k_1	Qe_{Calc} (mg/g)	R^2	k_2
Zn/Al-CH	201.174	80.682	79.947	0.9844	0.0020	106.383	0.9852	0.0002
Ni/Al-CH	201.174	87.879	87.680	0.9826	0.0023	106.383	0.9919	0.0002
Mg/Al-CH	201.174	115.152	129.658	0.9403	0.0022	125.000	0.9834	0.0002

The variation of initial concentration of CR (120, 140, 160, 180, and 200 mg/L) and adsorption temperature (30, 40, 50, and 60°C) using Zn/Al-CH, Ni/Al-CH, and Mg/Al-CH adsorbents aims to determine the thermodynamic parameters. Figure 7 shows an increase in adsorption capacity as the temperature used increases; this indicates the endothermic nature of the adsorption process. The maximum adsorption process occurs at a temperature of 333K as shown in Figure 7.

The adsorption capacity can determine the adsorption isotherm equation. The adsorption isotherm describes an interaction between the adsorbate and the adsorbent at equilibrium. Langmuir and Freundlich are the commonly used adsorption isotherm equations. The Langmuir isotherm is based on the assumption that adsorption takes place only in one layer (monolayer) where the active site has uniform energy (monolayer). The Freundlich isotherm, meanwhile, is assumed that adsorption takes place only on multilayer surfaces where adsorption increases with the increasing concentration and

takes place on adsorbents whose active sites have heterogeneous energies. The determination of the adsorption pattern can compare the value of linear regression (R^2) between Langmuir and Freundlich isotherms [22].
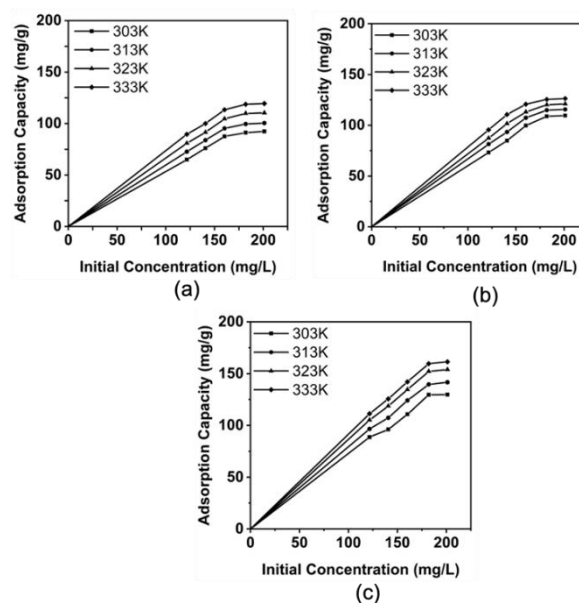

Figure 7. Effect of adsorption time on Zn/Al-CH (a), Ni/Al-CH (b), Mg/Al-CH ©

Table 2. Isotherm adsorption

Adsorbent	Adsorption Isotherm	Adsorption Constant	
Zn/Al-K	Langmuir	Qmax	181.818
		kL	0.031
		R^2	0.9636
	Freundlich	n	3.203
		kF	31.681
		R^2	0.8328
Ni/Al-K	Langmuir	Qmax	227.273
		kL	0.029
		R^2	0.9138
	Freundlich	n	1.879
		kF	17.302
		R^2	0.9073
Mg/Al-K	Langmuir	Qmax	344.828
		kL	0.067
		R^2	0.9560
	Freundlich	n	3.426
		kF	23.361
		R^2	0.8288

Based on the statement above, the adsorption process follows the Langmuir isotherm equation as seen from the R^2 value, which is closer to 1 for each adsorbent [23]. The maximum adsorption capacity of CR using Zn/Al-CH, Ni/Al-CH, and Mg/Al-CH were 181.818, 227.273, and 344.828 mg/g, respectively, as shown in Table 2. The CR adsorption process was more effective using Mg/Al-CH, which was characterized by the highest adsorption capacity value.

Thermodynamic parameters are used to determine whether the adsorption process takes place spontaneously or not based on the Gibbs free energy (ΔG) value. In this study, the

adsorption process occurred spontaneously [18], indicated by a negative Gibbs free energy (ΔG) value as shown in Table 3. The value of enthalpy (ΔH) and entropy (ΔS) in the adsorption process can also be seen in Table 2. The change in total heat energy indicates that the process occurs endothermic, which is known from the enthalpy value below +40 kJ/mol [24]. The degree of adsorption irregularity is positive and small where the greater the initial concentration of CR used, the smaller the entropy value and the degree of adsorption irregularity obtained [4].

Table 3. Thermodynamic adsorption

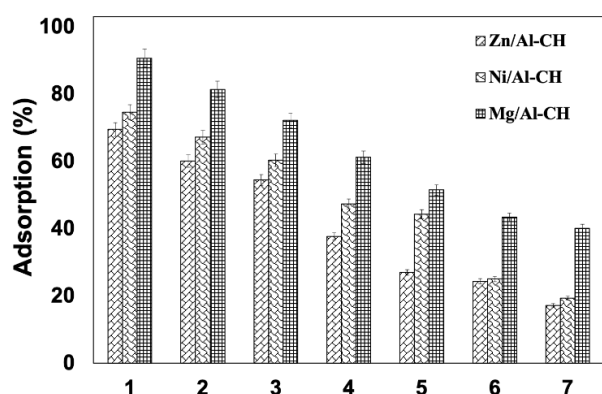| Adsorbent	T (K)	Q_e (mg/g)	ΔH (kJ/mol)	ΔS (J/mol K)	ΔG (kJ/mol)
Zn/Al-K	303	92.366	15.332	0.049	-0.445
	313	100.382			-0.046
	323	110.305			-0.537
	333	119.466			-1.028
Ni/Al-K	303	99.779	16.838	0.060	-1.244
	313	107.412			-1.840
	323	113.061			-2.437
	333	120.695			-3.034
Mg/Al-K	303	129.779	22.875	0.080	-1.503
	313	141.687			-2.308
	323	153.901			-3.112
	333	161.382			-3.917

Figure 8. Regeneration of Zn/Al-CH, Ni/Al-CH, and Mg/Al-CH

4. Conclusion

The manufacture of composites with LDH as a base material and a supporting material in the form of chitosan has been successfully synthesized. This is evidenced from the results of XRD characterization, which showed the appearance of LDH diffraction at an angle of 2θ = 11.63° (003); 23.00° (006); 35.16° (009); and 61.59° (110) and at angles of 2θ = 7.93° and 19.35° as the characteristic of chitosan. The adsorption capacity of CR using Zn/Al-CH, Ni/Al-CH, and Mg/Al-CH adsorbents were 181.818, 227.273, and 344.828 mg/g, respectively. The regeneration process showed the stability of Mg/Al-CH better than Zn/Al-CH and Ni/Al-CH to be adsorbent, which could be used repeatedly on CR adsorption.

Figure 8 shows the regeneration process of each adsorbent for seven cycles. The results showed that Mg/Al-CH was more

effectively used as an adsorbent. In addition to the higher adsorption capacity, Mg/Al-CH was also more stable to be reused in the CR adsorption process in an aqueous solution.

Table 4 shows the comparison of the absorption of CR from aqueous solutions using several adsorbents modified with chitosan. The adsorption capacity of CR in this study was greater than that of some of the adsorbents as shown in Table 4.

Table 4. Adsorption of CR by several adsorbents

Adsorbent	Adsorption capacity (mg/g)	Reference
Chitosan/Montmorillonite	54.52	[25]
Dialdehyde Microfibrillated Cellulose/Chitosan	152.5	[26]
Magnetic Chitosan Composite Microparticles	263.16	[27]
Chitosan Hydrobeads	93.71	[28]
Chitosan	78.90	[29]
Chitosan–Silica Composite	150	[30]
Chitosan Coated Magnetic Iron Oxide	56.66	[31]
Chitosan Hydrogel Core–Shell	124.97	[32]
Chitosan/Polyvinyl Alcohol/Tio₂	134	[33]
The Carboxymethyl-Chitosan-Montmorillonite	81.77	[34]
Cellulose/Chitosan	40	[3]
Chitosan Coated Luffa Fibers	20.37	[35]
Chitosan/Rectorite Composite	73.8	[36]
Zn/Al-CH	181.818	This Research
Ni/Al-CH	227.273	This Research
Mg/Al-CH	344.828	This Research

References

1. S. Amelia, M. Maryudi, *Application of Natural Zeolite in Methylene Blue Wastewater Treatment Process by Adsorption Method*, J. Bahan Alam Terbarukan 8 (2019) 144–147.

2. T. Taher, D. Rohendi, R. Mohadi, A. Lesbani, *Congo red dye removal from aqueous solution by acid-activated bentonite from sarolangun: kinetic, equilibrium, and thermodynamic studies*, Arab J. Basic Appl. Sci. 26 (2019) 125–136.

3. M. Li, Z. Wang, B. Li, *Adsorption behaviour of congo red by cellulose/chitosan hydrogel beads regenerated from ionic liquid*, Desalin. Water Treat. 57 (2016) 16970–16980.

4. P.M.S.B.N. Siregar, N.R. Palapa, A. Wijaya, E.S. Fitri, A. Lesbani, *Structural Stability of Ni/Al Layered Double Hydroxide Supported on Graphite and Biochar Toward Adorption of Congo Red*, Sci. Technol. Indones. 6 (2021) 85–95.

5. P. Hua et al., *Adsorption of acid green and procion red on a magnetic geopolymer based adsorbent: Experiments, characterization and theoretical treatment*, Chem. Eng. J. 383 (2020).

6. A.J. Sami, Y.N. Butt, S. Nasar, *Elimination of a Carcinogenic Anionic Dye Congo Red from Water Using Hydrogels Based on Chitosan, Acrylamide and Graphene Oxide*, J. Bioprocess. Biotech. 08 (2018).

7. C.M. Simonescu, A. Tătăruș, D.C. Culiță, N. Stănică, I.A. Ionescu, B. Butoi, A.M. Banici, *Comparative study of cofe2o4 nanoparticles and cofe2o4-chitosan composite for congo red and methyl orange removal by adsorption*, Nanomaterials 11 (2021) 1–24.

8. M.A. Zenasni, B. Meroufel, A. Merlin, B. George, *Adsorption of Congo Red from Aqueous Solution Using CTAB-Kaolin from Bechar Algeria*, J. Surf. Eng. Mater. Adv. Technol. 04 (2014) 332–341.

9. Z. Zhang, Y. Li, Q. Du, Q. Li, *Adsorption of Congo Red from Aqueous Solutions by Porous Soybean Curd Xerogels*, Polish J. Chem. Technol. 20 (2018) 95–102.

10. A. Hamzezadeh, Y. Rashtbari, S. Afshin, M. Morovati, M. Vosoughi, *Application of low-cost material for adsorption of dye from aqueous solution*, Int. J. Environ. Anal. Chem. 00 (2020) 1–16.

11. C. Nwodika, O.D. Onukwuli, *Adsorption Study of Kinetics and Equilibrium of Basic Dye on Kola Nut Pod Carbon*, Gazi Univ. J. Sci. 30 (2017) 86–102.

12. T.B. Nuria Fiol, *Adsorption on Activated Carbon from Olive Stones: Kinetics and Equilibrium of Phenol Removal from Aqueous Solution*, J. Chem. Eng. Process Technol. 04 (2013).

13. R. Mohadi, N.R. Palapa, R. Hartono, N. Hidayati, *The Utilization of Modified Chitosan from Shrimp Shell As Photodegradation of*, Sci. Technol. Indones. 6 (2021) 2–6.

14. W. Banana, P.C. Namasivayam, N. Kanchana, *Removal of Congo Red from Aqueous Solution*, Pertanika J. Sci. Techno! 1 (1993) 33–42.

15. C. Cojocaru, P. Samoila, P. Pascariu, *Chitosan-based magnetic adsorbent for removal of water-soluble anionic dye: Artificial neural network modeling and molecular docking insights*, Int. J. Biol. Macromol. 123 (2019) 587–599.

16. N.R. Palapa, T. Taher, B.R. Rahayu, R. Mohadi, A. Rachmat, A. Lesbani, *CuAl LDH/Rice husk biochar composite for enhanced adsorptive removal of cationic dye from aqueous solution*, Bull. Chem. React. Eng. Catal. 15 (2020) 525–537.

17. Normah, N.R. Palapa, T. Taher, R. Mohadi, H.P. Utami, A. Lesbani, *The Ability of Composite Ni / Al-carbon based Material Toward Readsorption of Iron (II) in Aqueous Solution*, Sci. Technol. Indones. 6 (2021).

18. Y.D. Ngapa, Y.E. Ika, *Indonesian Journal of Chemical Research*, Indones. J. Chem. Res. 8 (2020) 151–158.

19. M.M. AbdElhady, *Preparation and Characterization of Chitosan/Zinc Oxide Nanoparticles for Imparting Antimicrobial and UV Protection to Cotton Fabric*, Int. J. Carbohydr. Chem. 2012 (2012) 1–6.

20. S. Kumar, J. Koh, *Physiochemical, optical and biological activity of chitosan-chromone derivative for biomedical applications*, Int. J. Mol. Sci.

13 (2012) 6103–6116.

21. A.F. Badri, N.R. Palapa, R. Mohadi, A. Lesbani, *Cationic Dye Removal By Magnesium Aluminum - Biochar Composite From Aqueous Solution*, Int. J. Sci. Technol. Res. 9 (2020) 186–190.

22. A.F. Badri, P.M.S.B.N. Siregar, N.R. Palapa, R. Mohadi, M. Mardiyanto, A. Lesbani, *Mg-Al/Biochar Composite with Stable Structure for Malachite Green Adsorption from Aqueous Solutions*, Bull. Chem. React. Eng. Catal. 16 (2021) 149–160.

23. N.R. Palapa, T. Taher, A. Wijaya, A. Lesbani, *Modification of Cu / Cr Layered Double Hydroxide by Keggin Type Polyoxometalate as Adsorbent of Malachite Green from Aqueous Solution*, Sci. Technol. Indones. 6 (2021).

24. L. Wang, A. Wang, *Adsorption characteristics of Congo Red onto the chitosan/montmorillonite nanocomposite*, J. Hazard. Mater. 147 (2007) 979–985.

25. X. Zheng et al., *Efficient removal of anionic dye (Congo red) by dialdehyde microfibrillated cellulose/chitosan composite film with significantly improved stability in dye solution*, Int. J. Biol. Macromol. 107 (2018) 283–289.

26. P. Wang, T. Yan, L. Wang, *Removal of congo red from aqueous solution using magnetic chitosan composite microparticles*, BioResources 8 (2013) 6026–6043.

27. S. Chatterjee, S. Chatterjee, B.P. Chatterjee, A.R. Das, A.K. Guha, *Adsorption of a model anionic dye, eosin Y, from aqueous solution by chitosan hydrobeads*, J. Colloid Interface Sci. 288 (2005) 30–35.

28. L. Wang, A. Wang, *Adsorption properties of congo red from aqueous solution onto N,O-carboxymethyl-chitosan*, Bioresour. Technol. 99 (2008) 1403–1408.

29. J. Wang, Q. Zhou, D. Song, B. Qi, Y. Zhang, Y. Shao, Z. Shao, *Chitosan–silica composite aerogels: preparation, characterization and Congo red adsorption*, J. Sol-Gel Sci. Technol. 76 (2015) 501–509.

30. H. Zhu, M. Zhang, Y. Liu, L. Zhang, R. Han, *Study of congo red adsorption onto chitosan coated magnetic iron oxide in batch mode*, Desalin. Water Treat. 37 (2012) 46–54.

31. S. Chatterjee, T. Chatterjee, S.R. Lim, S.H. Woo, *Effect of the addition mode of carbon nanotubes for the production of chitosan hydrogel core-shell beads on adsorption of Congo red from aqueous solution*, Bioresour. Technol. 102 (2011) 4402–4409.

32. U. Habiba, J.J.L. Lee, T.C. Joo, B.C. Ang, A.M. Afifi, *Degradation of methyl orange and congo red by using chitosan/polyvinyl alcohol/TiO 2 electrospun nanofibrous membrane*, Int. J. Biol. Macromol. 131 (2019) 821–827.

33. H. Zhang, J. Ma, F. Wang, Y. Chu, L. Yang, M. Xia, *Mechanism of carboxymethyl chitosan hybrid montmorillonite and adsorption of Pb(II) and Congo red by CMC-MMT organic-inorganic hybrid composite*, Int. J. Biol. Macromol. 149 (2020) 1161–1169.

34. C. Seedao, T. Rachphirom, M. Phiromchoei, W. Jangiam, *Anionic dye adsorption from aqueous solutions by chitosan coated luffa fibers*, ASEAN J. Chem. Eng. 18 (2018) 31–40.

35. T. Feng, L. Xu, *Adsorption of congo red from aqueous solution onto chitosan/rectorite composite*, Adv. Mater. Res. 690 693 (2013) 438–441.